



Frustrations and complexity in classical and quantum spin systems

Mikhail Katsnelson

Main collaborators

Andrey Bagrov, Tom Westerhout, Askar Iliasov, Achille Mauri, Alex Kolmus, Bert Kappen, Alex Khajetoorians, Daniel Wegner and others, Radboud University

Olle Eriksson, Anders Bergman, Diana Iușan and others, Uppsala University

Vladimir Mazurenko, Ilia Iakovlev, Oleg Sotnikov, Ural Federal University

Vitaly Vanchurin, University of Minnesota

Eugene Koonin, Yuri Wolf, National Center for Biotechnology Information, Bethesda

Yuri Gornostyrev, Institute of Metal Physics, Ekaterinburg

Alessandro Principi, Manchester University

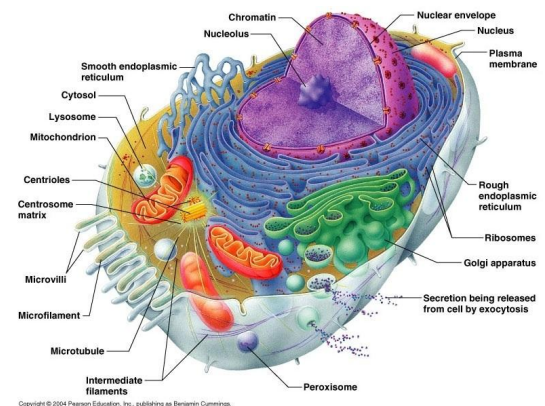
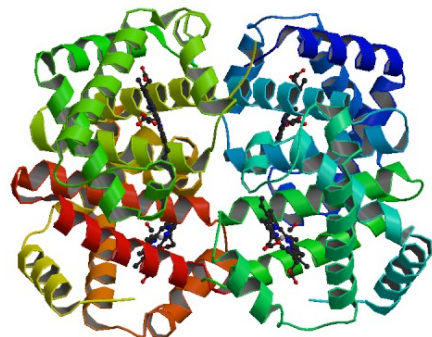
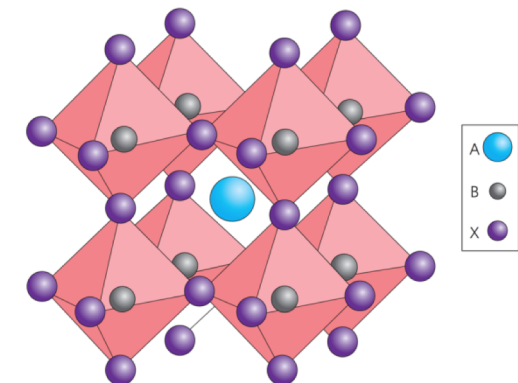
Outline

- **Introduction**
- **Pattern formation in physics: magnetic patterns as an example**
- **Multiscale structural complexity**
- **Self-induced glassiness and beyond: the role of frustration**
- **Experimental realization: elemental Nd**
- **Complexity of quantum frustrated systems**
- **Frustrations and complexity beyond materials science: machine learning, biological evolution and all that**

Complexity

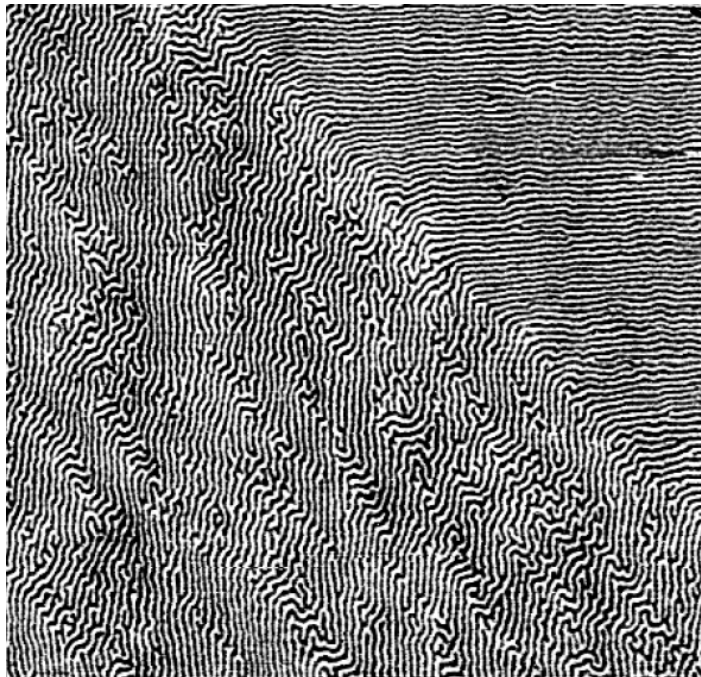
Schrödinger: life substance is “aperiodic crystal” (modern formulation – Laughlin, Pines and others – glass)

Intuitive feeling: crystals are simple, biological structures are complex



Origin and evolution of life: origin of complexity?

Complexity (“patterns”) in inorganic world

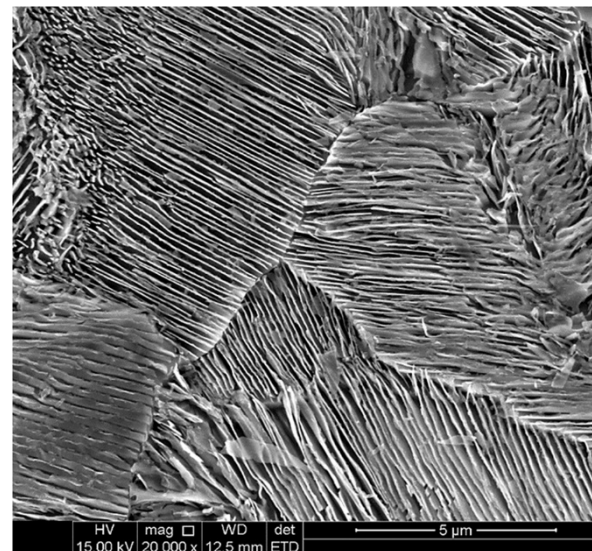


Stripe domains in ferromagnetic thin films

Microstructures in metals and alloys



Stripes on a beach in tide zone



Pearlitic structure in rail steel
(Sci Rep 9, 7454 (2019))

Do we understand this? No, or, at least, not completely

Magnetic patterns

Example: strip domains in thin ferromagnetic films

PHYSICAL REVIEW B 69, 064411 (2004)

Magnetization and domain structure of bcc $\text{Fe}_{81}\text{Ni}_{19}/\text{Co}$ (001) superlattices

R. Bručas, H. Hafermann, M. I. Katsnelson, I. L. Soroka, O. Eriksson, and B. Hjörvarsson

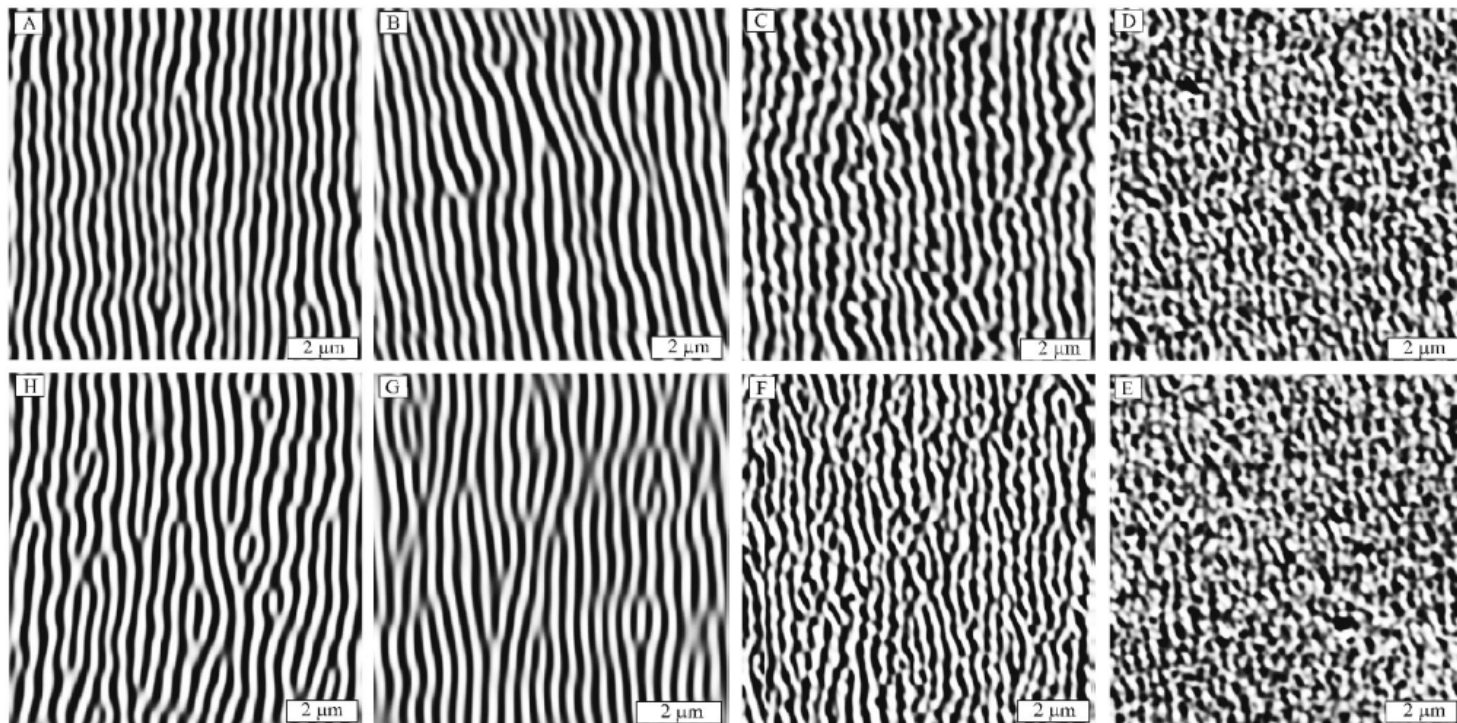


FIG. 2. The MFM images of the 420 nm thick $\text{Fe}_{81}\text{Ni}_{19}/\text{Co}$ superlattice at different externally applied in-plane magnetic fields: (a)—virgin (nonmagnetized) state; (b), (c), (d)—increasing field 8.3, 30, and 50 mT; (e), (f), (g)—decreasing field 50, 30, 8.3 mT; (h)—in remanent state.

Magnetic patterns II

Europhys. Lett., **73** (1), pp. 104–109 (2006)

DOI: 10.1209/epj/i2005-10367-8

Topological defects, pattern evolution, and hysteresis
in thin magnetic films

P. A. PRUDKOVSKII¹, A. N. RUBTSOV¹ and M. I. KATSNELSON²

$$H = \int \left(\frac{J_x}{2} \left(\frac{\partial \mathbf{m}}{\partial x} \right)^2 + \frac{J_y}{2} \left(\frac{\partial \mathbf{m}}{\partial y} \right)^2 - \frac{K}{2} m_z^2 - hm_y \right) d^2r + \\ + \frac{Q^2}{2} \int \int m_z(\mathbf{r}) \left(\frac{1}{|\mathbf{r}-\mathbf{r}'|} - \frac{1}{\sqrt{d^2 + (\mathbf{r}-\mathbf{r}')^2}} \right) m_z(\mathbf{r}') d^2r d^2r'.$$

Competition of exchange interactions (want homogeneous ferromagnetic state) and magnetic dipole-dipole interactions (want total magnetization equal to zero)

Magnetic patterns III

Classical Monte Carlo simulations

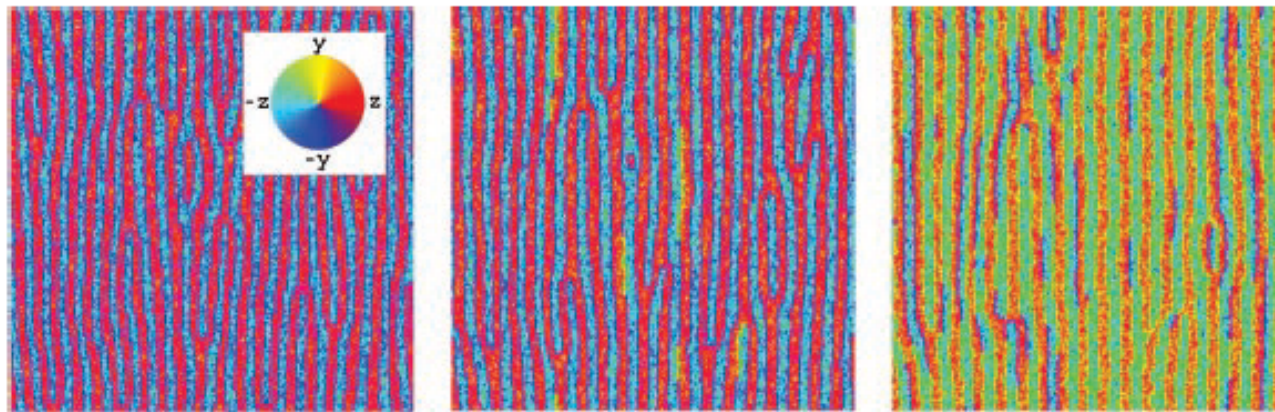


Fig. 2 – Snapshots of the stripe-domain system with the two-component order parameter at several points of the hysteresis loop for $\beta = 1$. The magnetic field is $h = 0$, $h = 0.3$, and $h = 0.6$, from left to right. The inset shows the color legend for the orientation of local magnetization.

We know the Hamiltonian and it is not very complicated

How to **describe** patterns and how to **explain** patterns?

What is complexity?

- Something that we immediately recognize when we see it, but very hard to define quantitatively

“I know it when I see it” (US Supreme Court Justice Potter Stewart, on obscenity)

- S. Lloyd, “Measures of complexity: a non-exhaustive list” – 40 different definitions
- Can be roughly divided into two categories:
 - computational/descriptive complexities (“ultraviolet”)
 - effective/physical complexities (“infrared” or inter-scale)

Our definition: Multiscale structural complexity

Multi-scale structural complexity of natural patterns

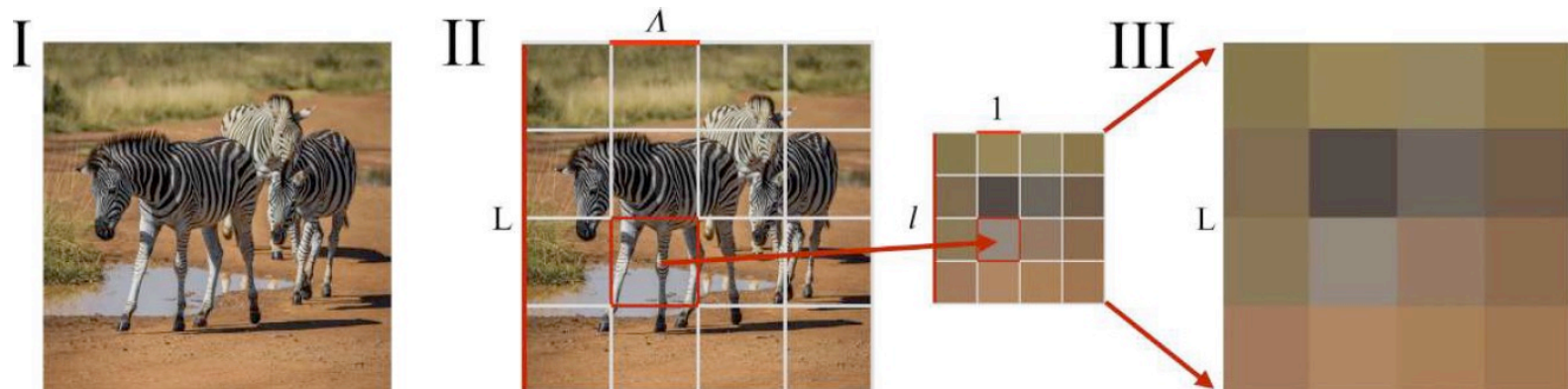
PNAS 117, 30241 (2020)

Andrey A. Bagrov^{a,b,1,2}, Ilia A. Iakovlev^{b,1}, Askar A. Iliasov^c, Mikhail I. Katsnelson^{c,b}, and Vladimir V. Mazurenko^b

The idea: Complexity is dissimilarity at various scales

$f(x)$ multidimensional pattern $f_\Lambda(x)$ its coarse-grained version

Complexity is related to distances between $f_\Lambda(x)$ and $f_{\Lambda+d\Lambda}(x)$



$$\begin{aligned}\Delta_\Lambda &= |\langle f_\Lambda(x) | f_{\Lambda+d\Lambda}(x) \rangle - \\ &\frac{1}{2} (\langle f_\Lambda(x) | f_\Lambda(x) \rangle + \langle f_{\Lambda+d\Lambda}(x) | f_{\Lambda+d\Lambda}(x) \rangle)| = \\ &\frac{1}{2} |\langle f_{\Lambda+d\Lambda}(x) - f_\Lambda(x) | f_{\Lambda+d\Lambda}(x) - f_\Lambda(x) \rangle|,\end{aligned}$$

$$\begin{aligned}\langle f(x) | g(x) \rangle &= \int_D dx f(x) g(x) \\ c &= \sum_\Lambda \frac{1}{d\Lambda} \Delta_\Lambda \rightarrow \int \left| \left\langle \frac{\partial f}{d\Lambda} \middle| \frac{\partial f}{d\Lambda} \right\rangle \right| d\Lambda, \text{ as } d\Lambda \rightarrow 0\end{aligned}$$

Multiscale structural complexity II

Solution of ink drop in water:

Entropy should grow but complexity is not

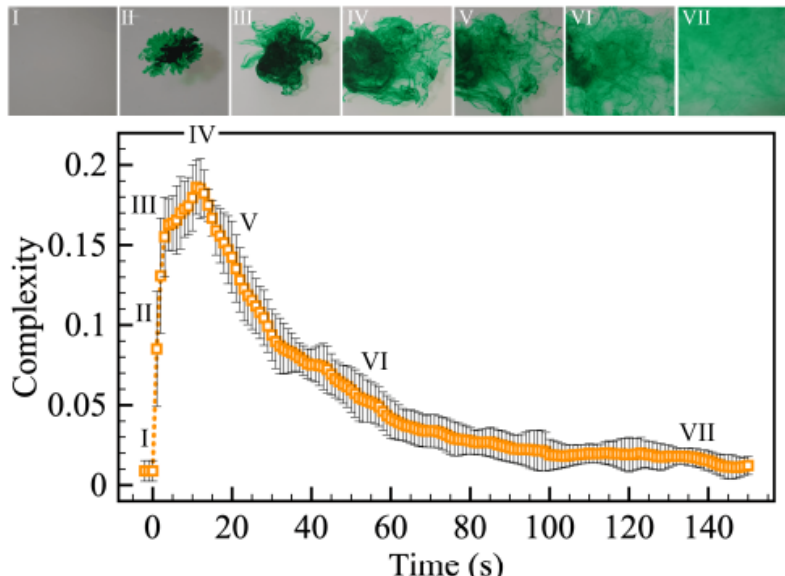


FIG. 7. The evolution of the complexity during the process of dissolving a food dye drop of 0.3 ml in water at 31°C.

And many other applications including biology and psychology

Magnetic patterns

$$H = -J \sum_{nn'} \mathbf{S}_n \mathbf{S}_{n'} - D \sum_{nn'} [\mathbf{S}_n \times \mathbf{S}_{n'}] - \sum_n B S_n^z$$

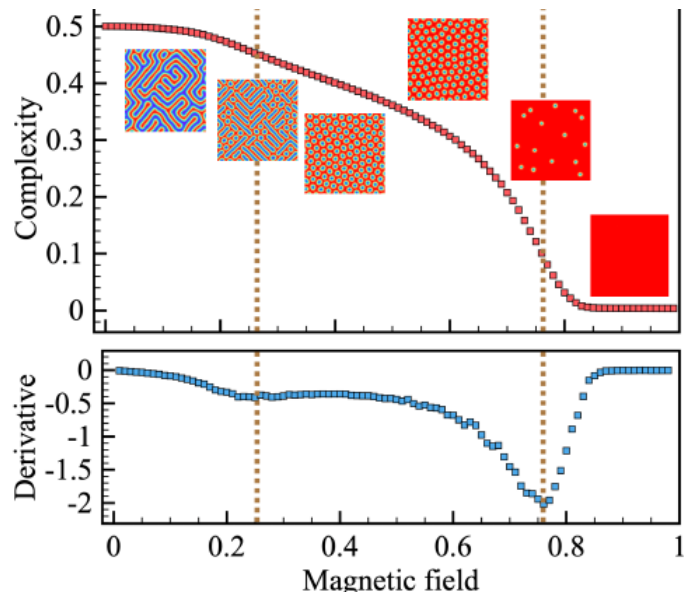
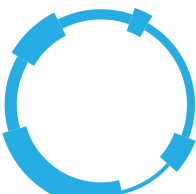


FIG. 4. (a) Magnetic field dependence of the complexity obtained from the simulations with spin Hamiltonian containing DM interaction with $J = 1$, $|D| = 1$, $T = 0.02$. The error bars are smaller than the symbol size. (b) Complexity derivative we used for accurate detection of the phases boundaries.

Derivative detects changes of regime



Long range segmentation of prokaryotic genomes by gene age and functionality

Yuri I. Wolf ^①, Ilya V. Schurov ^②, Kira S. Makarova ^①, Mikhail I. Katsnelson ^② and Eugene V. Koonin ^{①,*}

Certification of quantum states

Certification of quantum states with hidden structure of their bitstrings

npj Quantum Information (2022) 8:41

O. M. Sotnikov  , I. A. Iakovlev  , A. A. Iliasov ², M. I. Katsnelson  , A. A. Bagrov   ^{2,3} and V. V. Mazurenko   

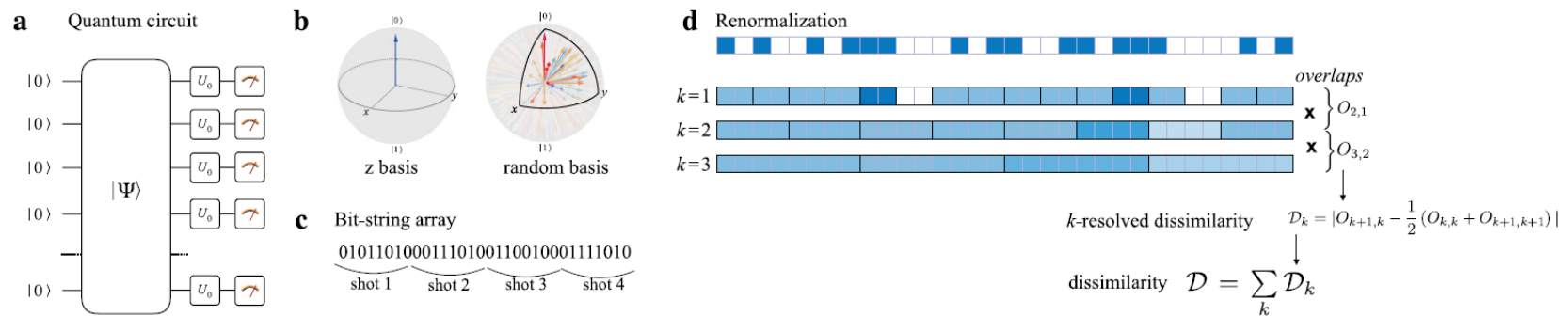


Fig. 1 Protocol for computing dissimilarity of a quantum state. **a** First, one prepares a state on a quantum device and chooses the measurement basis by applying rotational gates U_0 to individual qubits. **b** In this paper, we work with σ^z and random bases whose Bloch sphere representations are shown in the picture. We say that the set of measurements is performed in a random basis if, for each shot of measurement, a random vector belonging to the highlighted sector of the Bloch sphere is uniformly sampled and the corresponding parameters of gate U_0 are applied. **c** A number of measurements is performed and their outcomes — bitstrings of length N — are then stacked together in a one-dimensional binary array of length $N \times N_{\text{shots}}$ that serves as a classical representation of the quantum state. **d** The array is coarse-grained in several steps (indexed with k). Different schemes can be employed, but here we use plain averaging with fixed filter size Λ . In the picture, blue and white squares in the top line correspond to '0' and '1' bits in the array shown in (c), and black rectangles depict the blocks where averaging occurs at every step of coarse-graining. Overlap-based dissimilarities D_k between subsequent arrays are computed and summed up to the overall dissimilarity \mathcal{D} . See Methods section for more details.

First make at least two complementary measurements, then analyze the measurement results (relation to Bohr's complementarity principle)

Certification of quantum states II

Two-dimensional map can be used to characterize the type of quantum states

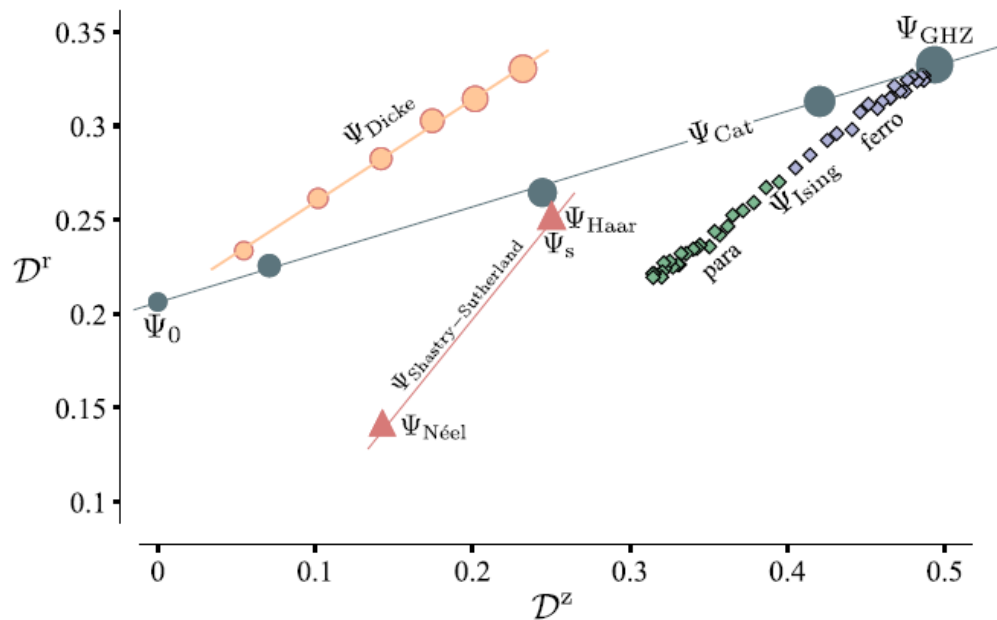


Fig. 10 Dissimilarity map. Low-dimensional representation of the 16-qubit quantum states studied in this work with respect to their dissimilarity calculated in σ^z and random bases. Ψ_0 , Ψ_s , Ψ_{Haar} denote the trivial $|0\rangle^{\otimes N}$, the singlet and the random quantum states, respectively.

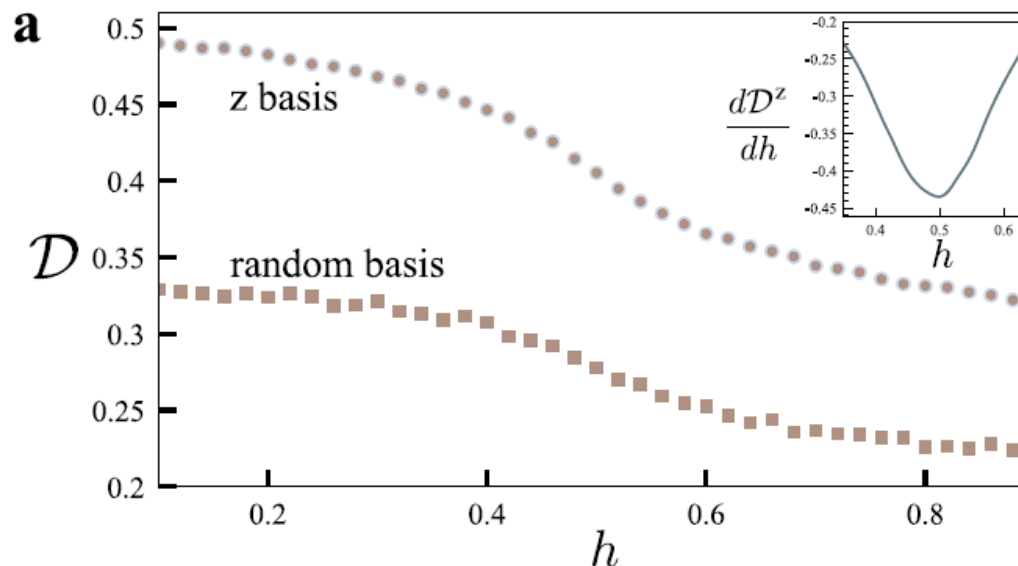
Certification of quantum states III

One can characterize a type of quantum states and, again, find (quantum) critical point

Ising in transverse field

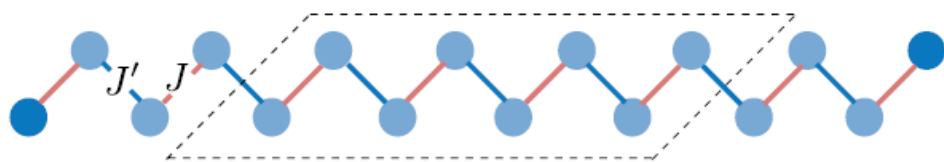
$$H = J \sum_{ij} \hat{S}_i^z \hat{S}_j^z + h \sum_i \hat{S}_i^x$$

1D chain; quantum critical point at $h_c = 0.5|J|$



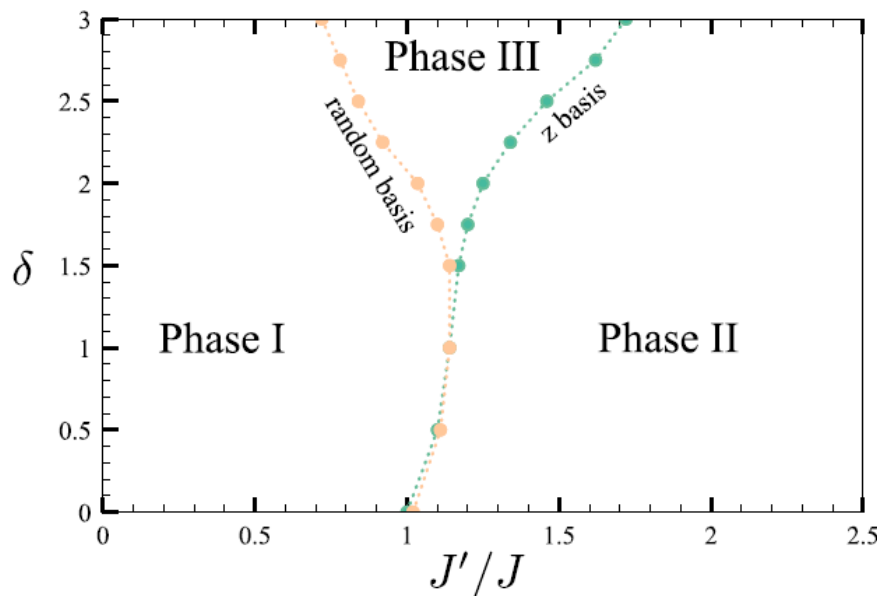
Certification of quantum states IV

The way to detect topological phases

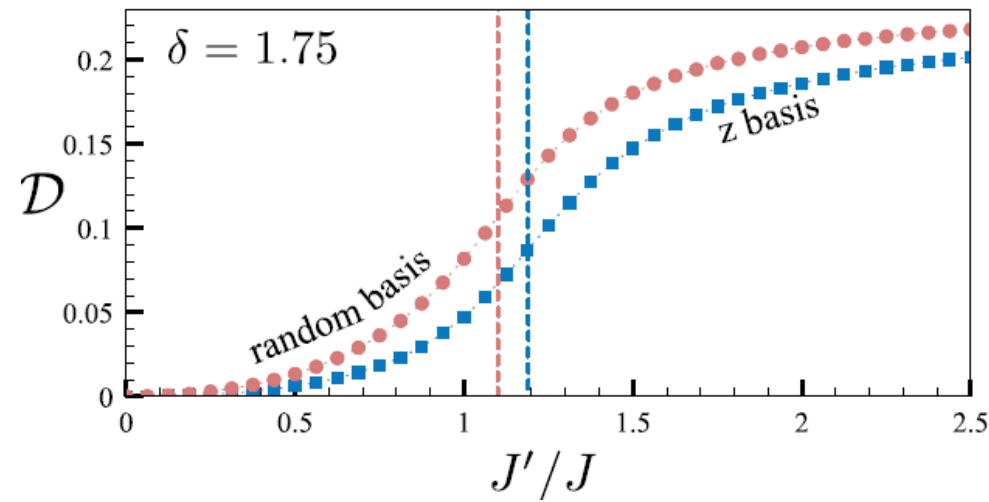


$$H_{XXZ} = J \sum_{ij \in \mathcal{O}} (\hat{S}_i^x \hat{S}_j^x + \hat{S}_i^y \hat{S}_j^y + \delta \hat{S}_i^z \hat{S}_j^z) + J' \sum_{ij \in \mathcal{E}} (\hat{S}_i^x \hat{S}_j^x + \hat{S}_i^y \hat{S}_j^y + \delta \hat{S}_i^z \hat{S}_j^z)$$

Three different phases: trivial (I), topological (II), antiferromagnetic (III)



Phase diagram constructed from dissimilarity (MSC), from maxima of its derivatives



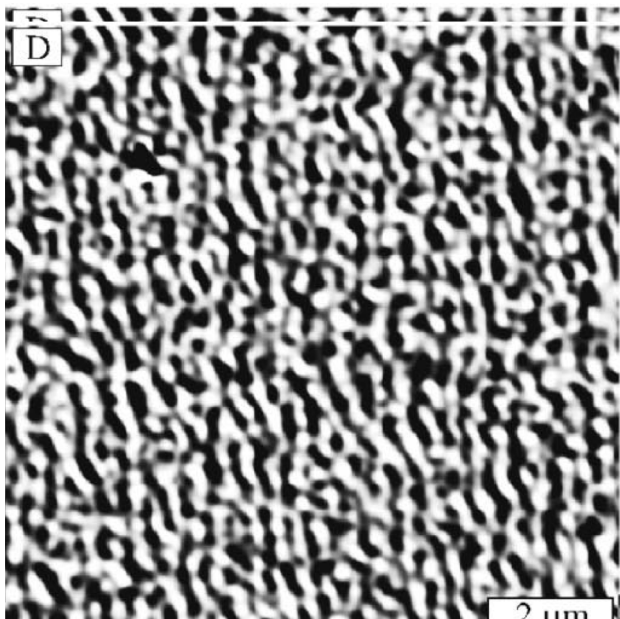
Dissimilarities with different basis show different phase boundaries

Competing interactions and self-induced spin glasses

Special class of patterns: “chaotic” patterns

Hypothesis: a system wants to be modulated but cannot decide in which direction

PHYSICAL REVIEW B 69, 064411 (2004)



$$E_m = \int \int d\mathbf{r} d\mathbf{r}' m(\mathbf{r}) m(\mathbf{r}') \left[\frac{1}{|\mathbf{r} - \mathbf{r}'|} - \frac{1}{\sqrt{(\mathbf{r} - \mathbf{r}')^2 + D^2}} \right] \\ = 2\pi \sum_{\mathbf{q}} m_{\mathbf{q}} m_{-\mathbf{q}} \frac{1 - e^{-qD}}{q}, \quad (13)$$

where $m_{\mathbf{q}}$ is a two-dimensional Fourier component of the magnetization density. At the same time, the exchange energy can be written as

$$E_{exch} = \frac{1}{2} \alpha \sum_{\mathbf{q}} q^2 m_{\mathbf{q}} m_{-\mathbf{q}}, \quad (14)$$

so there is a finite value of the wave vector $q = q^*$ found from the condition

$$\frac{d}{dq} \left(2\pi \frac{1 - e^{-qD}}{q} + \frac{1}{2} \alpha q^2 \right) = 0 \quad (15)$$

Self-induced spin glasses II

PHYSICAL REVIEW B 93, 054410 (2016)

PRL 117, 137201 (2016)

PHYSICAL REVIEW LETTERS

week ending
23 SEPTEMBER 2016

Stripe glasses in ferromagnetic thin films

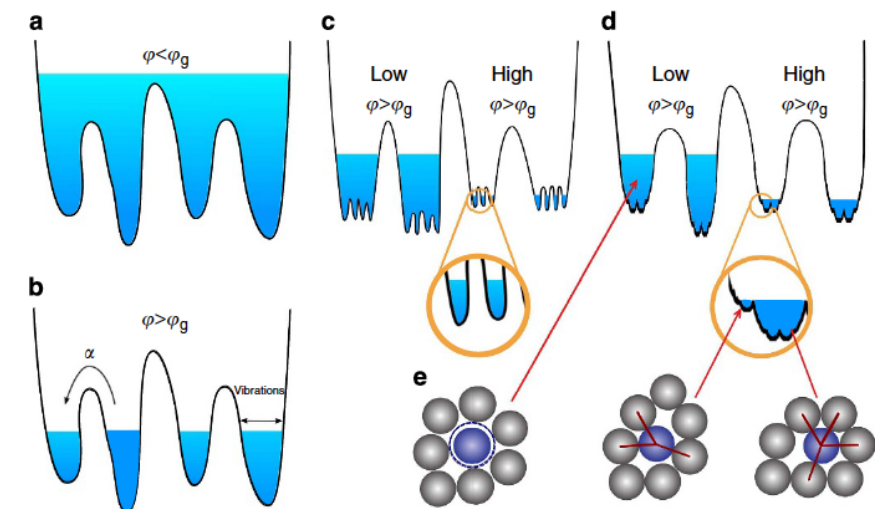
Alessandro Principi* and Mikhail I. Katsnelson

Self-Induced Glassiness and Pattern Formation in Spin Systems Subject to Long-Range Interactions

Alessandro Principi* and Mikhail I. Katsnelson

Development of idea of stripe glass, J. Schmalian and P. G. Wolynes, PRL 2000

Glass: a system with an energy landscape characterizing by infinitely many local minima, with a broad distribution of barriers, relaxation at “any” time scale and **aging** (at thermal cycling you never go back to *exactly* the same state)



Picture from P. Charbonneau et al,

DOI: 10.1038/ncomms4725

Intermediate state between equilibrium and non-equilibrium, opportunity for history and memory (“stamp collection”)

Self-induced spin glasses III

One of the ways to describe: R. Monasson, PRL 75, 2847 (1995)

$$\mathcal{H}_\psi[m, \lambda] = \mathcal{H}[m, \lambda] + g \int d\mathbf{r} [m(\mathbf{r}) - \psi(\mathbf{r})]^2$$

The second term describes attraction of our physical field $m(\mathbf{r})$
to some external field $\psi(\mathbf{r})$

If the system can be glued, with infinitely small interaction g , to macroscopically large number of configurations it should be considered as a glass

Then we calculate $F_g = \frac{\int \mathcal{D}\psi Z[\psi] F[\psi]}{\int \mathcal{D}\psi Z[\psi]}$ and see whether the limits

$F_{\text{eq}} = \lim_{N \rightarrow \infty} \lim_{g \rightarrow 0} F_g$ and $F = \lim_{g \rightarrow 0} \lim_{N \rightarrow \infty} F_g$ are different

If yes, this is **self-induced glass**

No disorder is needed (contrary to traditional view on spin glasses)

Self-induced spin glasses IV

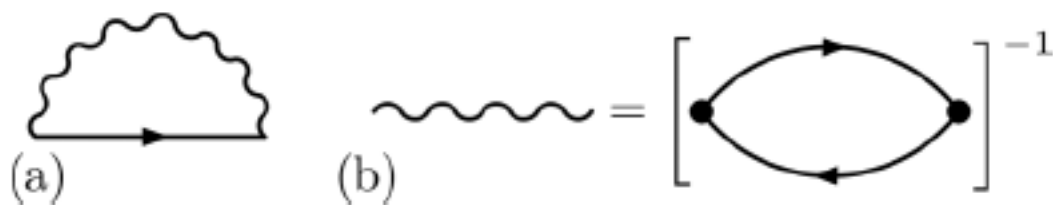
PHYSICAL REVIEW B 93, 054410 (2016)

Stripe glasses in ferromagnetic thin films

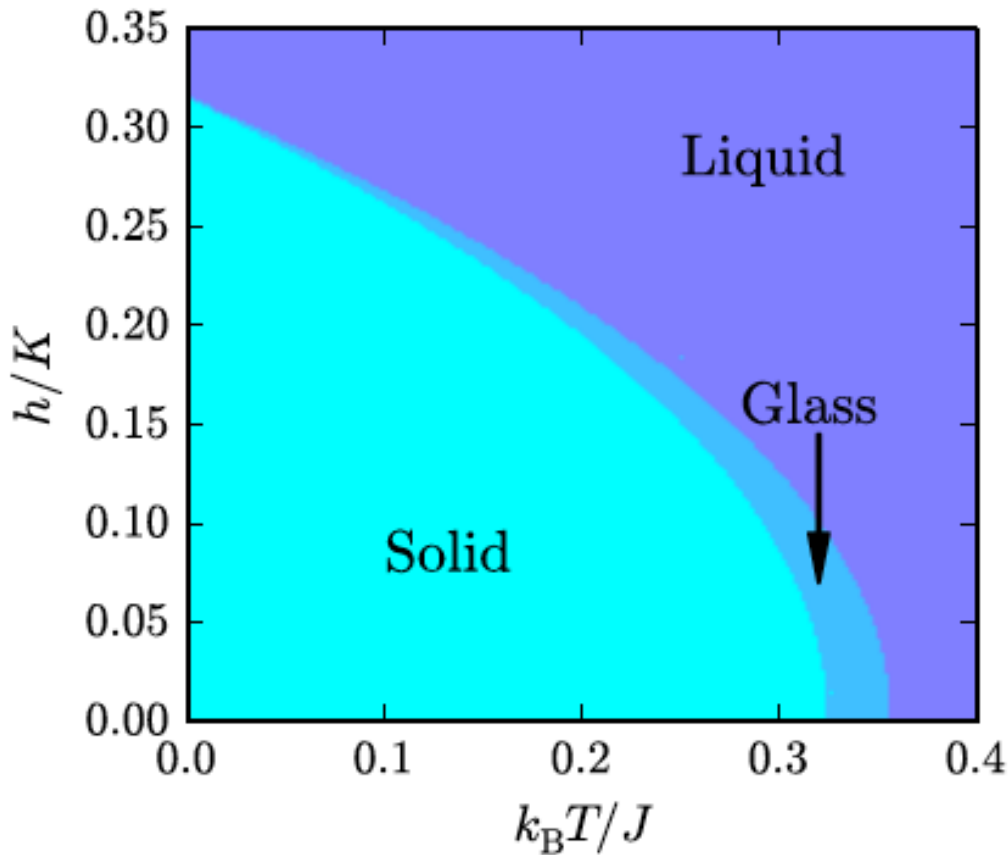
Alessandro Principi* and Mikhail I. Katsnelson

$$\begin{aligned}\mathcal{H}[\mathbf{m}, \lambda] = & \int d\mathbf{r} \{ J[\partial_i m_j(\mathbf{r})]^2 - K m_z^2(\mathbf{r}) - 2\mathbf{h}(\mathbf{r}) \cdot \mathbf{m}(\mathbf{r}) \} \\ & + \frac{Q}{2\pi} \int d\mathbf{r} d\mathbf{r}' m_z(\mathbf{r}) \\ & \times \left[\frac{1}{|\mathbf{r} - \mathbf{r}'|} - \frac{1}{\sqrt{d^2 + |\mathbf{r} - \mathbf{r}'|^2}} \right] m_z(\mathbf{r}') \\ & + \int d\mathbf{r} \{ \lambda(\mathbf{r}) [\mathbf{m}^2(\mathbf{r}) - 1] \}. \quad (1)\end{aligned}$$

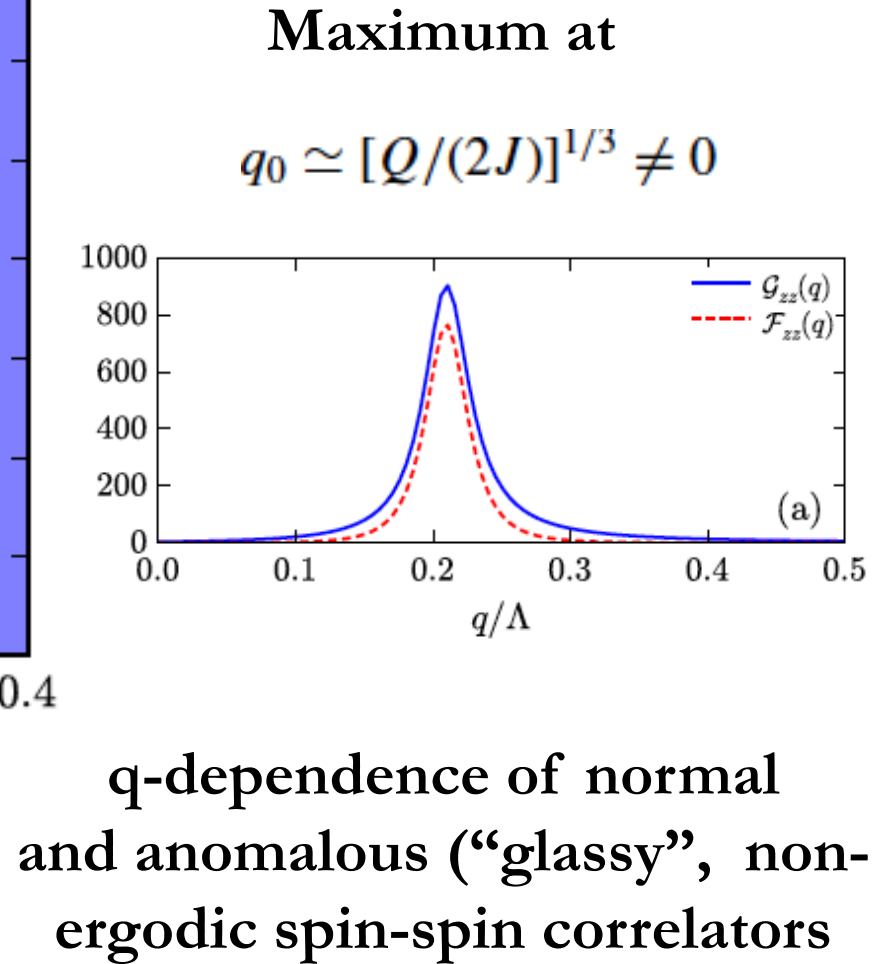
Self-consistent screening approximation for spin propagators



Self-induced spin glasses V



Phase diagram



Glassiness without disorder?

Giorgio Parisi, Nobel Prize in physics 2021

"for the discovery of the interplay of disorder and fluctuations in physical systems from atomic to planetary scales."



Actually, disorder may be not needed, frustrations are enough
(self-induced spin glass state in Nd)

Can we have something more or less exactly solvable?! – Yes!

PHYSICAL REVIEW B **109**, 144414 (2024)

Frustrated magnets in the limit of infinite dimensions: Dynamics and disorder-free glass transition

Achille Mauri * and Mikhail I. Katsnelson †

Institute for Molecules and Materials, Radboud University, Heijendaalseweg 135, 6525 AJ Nijmegen, The Netherlands



(Received 16 November 2023; accepted 27 March 2024; published 18 April 2024)

The prototype theory: dynamical mean-field theory (DMFT) for strongly correlated systems (Metzner, Vollhardt, Georges, Kotliar and others)

Glassiness in infinite dimensions

Frustrations are necessary

$$H = -\frac{1}{2} \sum_{i,j} J_{ij}^{\alpha\beta} S_i^\alpha S_j^\beta + \sum_i V(\mathbf{S}_i)$$

$$\mathbf{S}_i^2 = S_i^\alpha S_i^\alpha = 1$$

The limit of large dimensionality d

$$J_{ij}^{\alpha\beta} = [f^{\alpha\beta}(\hat{t}/\sqrt{2d})] \quad \text{e.g.}$$

$$f^{\alpha\beta}(x) = J_0^{\alpha\beta} + J_1^{\alpha\beta}x + J_2^{\alpha\beta}x^2 + J_4^{\alpha\beta}x^4 \quad \text{means}$$

$$J_{ij}^{\alpha\beta} = J_0^{\alpha\beta} \delta_{ij} + \frac{J_1^{\alpha\beta}}{\sqrt{2d}} t_{ij} + \frac{J_2^{\alpha\beta}}{2d} \sum_k t_{ik} t_{kj}$$

$$+ \frac{J_4^{\alpha\beta}}{4d^2} \sum_{k,l,m} t_{ik} t_{kl} t_{lm} t_{mj} .$$

The simplest frustrated model:

$$f^{\alpha\beta}(\varepsilon) = \delta^{\alpha\beta} f(\varepsilon) \quad f(\varepsilon) = J(\varepsilon^2 - 1)$$

Mean-field ordering temperature tends to zero at $d \rightarrow \infty$ in this model

Glassiness in infinite dimensions II

Cavity construction and mapping on effective single impurity

Purely dissipative Langevin dynamics

$$\begin{aligned}\dot{\mathbf{S}}_i &= -\mathbf{S}_i \times (\mathbf{S}_i \times (\mathbf{N}_i + \boldsymbol{\nu}_i)) \\ &= \mathbf{N}_i + \boldsymbol{\nu}_i - \mathbf{S}_i(\mathbf{S}_i \cdot (\mathbf{N}_i + \boldsymbol{\nu}_i))\end{aligned}$$

$$\mathbf{N}_i = -\frac{\partial H}{\partial \mathbf{S}_i} = \mathbf{b}_i + \mathbf{F}_i \quad b_i^\alpha = \sum_j J_{ij}^{\alpha\beta} S_j^\beta \quad F^\alpha(\mathbf{S}_i) = -\partial V(\mathbf{S}_i)/\partial S_i^\alpha$$

$$\langle \nu_i^\alpha(t) \nu_j^\beta(t') \rangle = 2k_B T \delta^{\alpha\beta} \delta_{ij} \delta(t - t')$$

Exactly mapped to a single-impurity dynamics with nonlocal in time “memory function”

Edwards-Anderson criterion of glassiness (local spin-spin correlation function tends to nonzero value in the limit of infinite time difference)

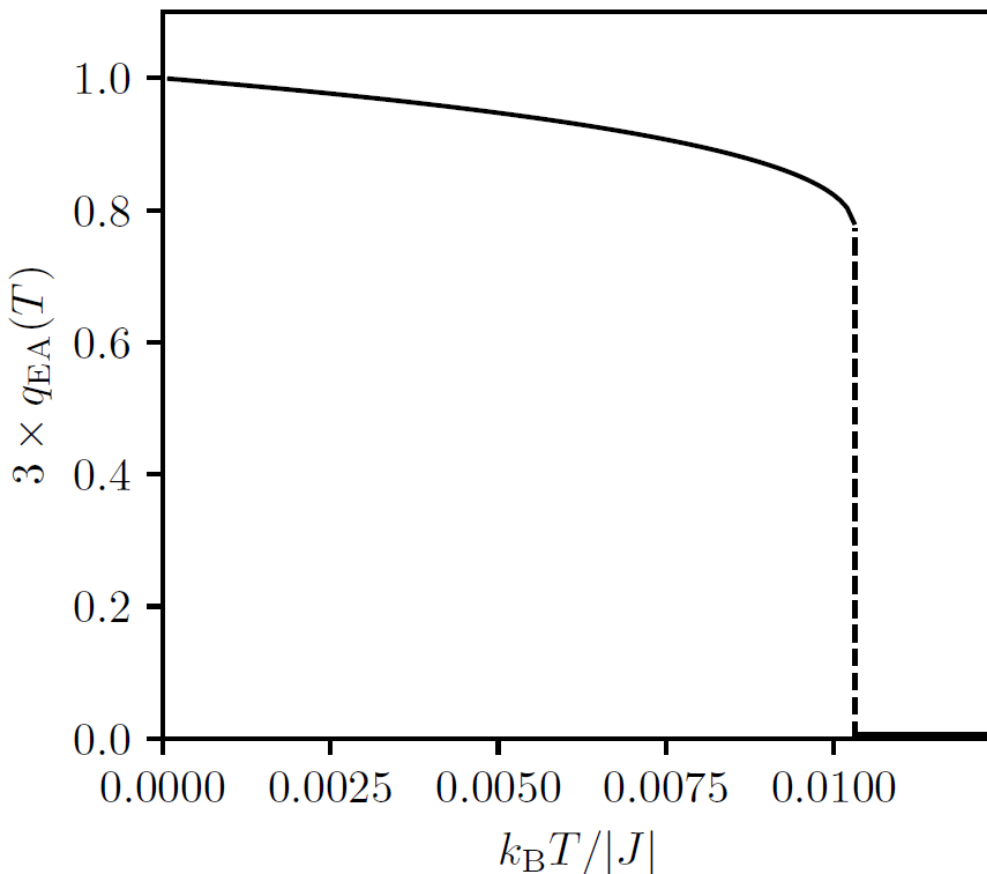
$$3q_{\text{EA}}(T) = \lim_{|t-t'| \rightarrow \infty} \langle S^\alpha(t) S^\alpha(t') \rangle$$

Glassiness in infinite dimensions III

Isotropic model $f(\varepsilon) = J(\varepsilon^2 - 1)$

nonzero below the glass transition temperature $T_g \simeq 0.0103|J|/k_B$

First-order transition $q_{EA}(T_g) \simeq 0.2575$



Glassiness without disorder is
theoretically possible!

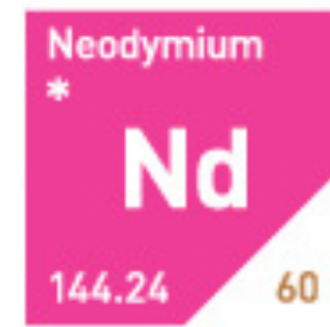
Experimental observation of self-induced spin glass state: elemental Nd

Self-induced spin glass state in elemental and crystalline neodymium

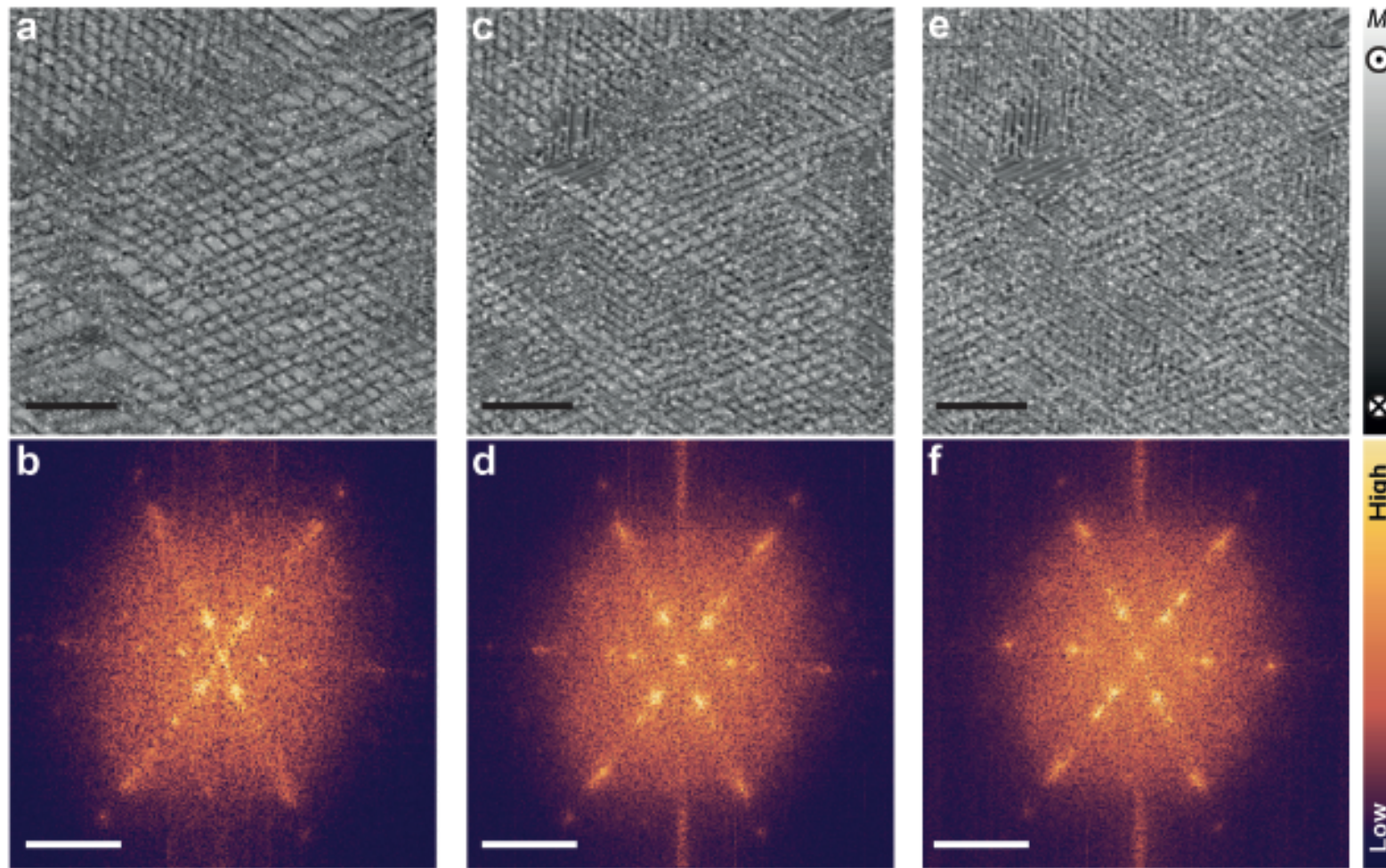
Science **368**, 966 (2020)

Umut Kamber, Anders Bergman, Andreas Eich, Diana Iușan, Manuel Steinbrecher, Nadine Hauptmann, Lars Nordström, Mikhail I. Katsnelson, Daniel Wegner*, Olle Eriksson, Alexander A. Khajetoorians*

Spin-polarized STM experiment, Radboud University



Magnetic structure: local correlations

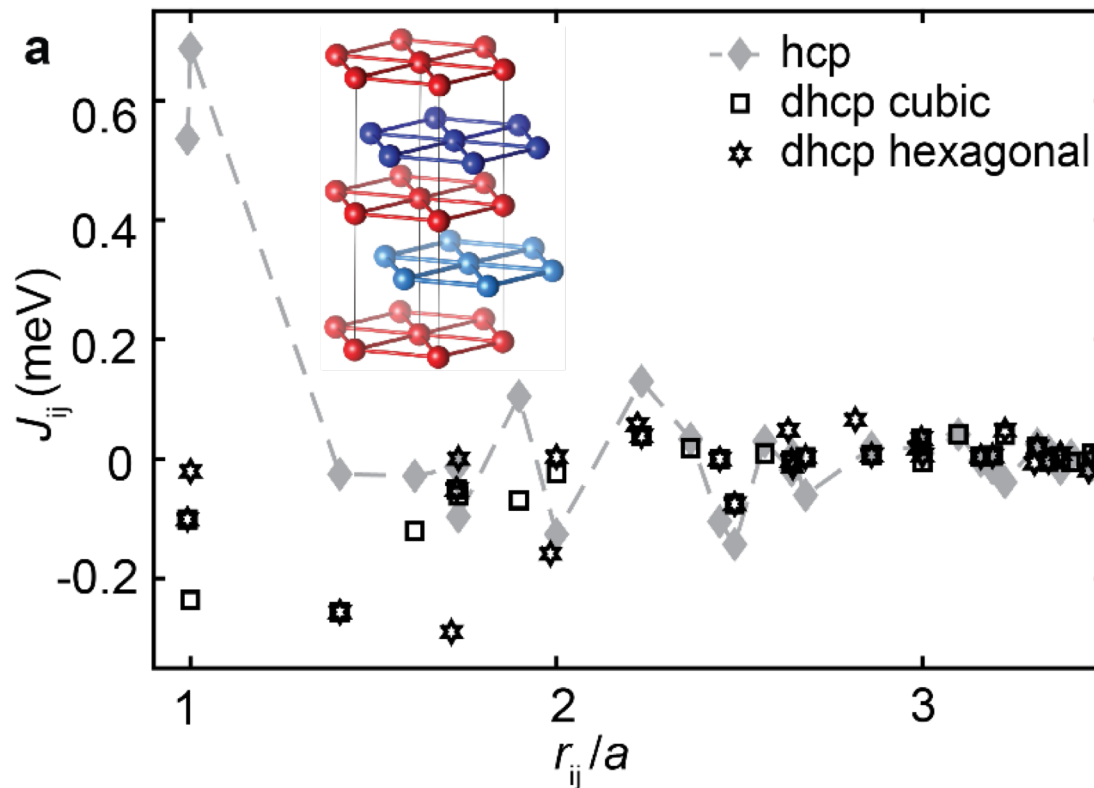


The most important observation: **aging**. At thermocycling (or cycling magnetic field) the magnetic state is not exactly reproduced

Ab initio: magnetic interactions in bulk Nd

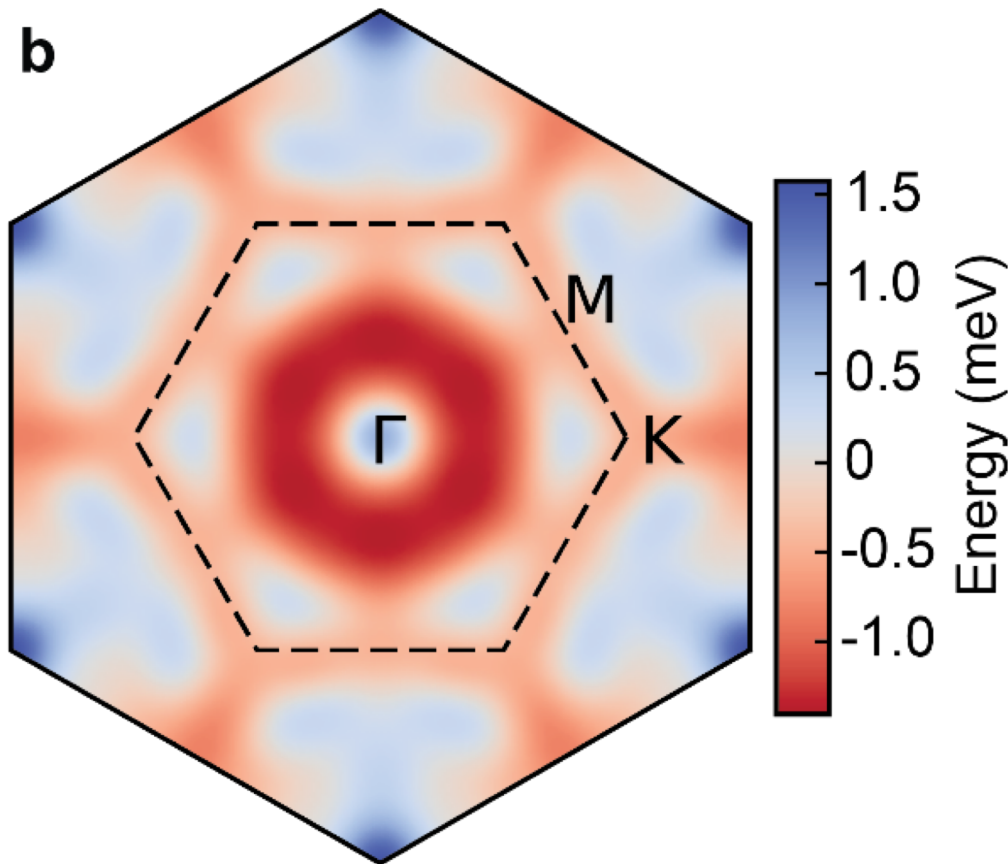
Method: magnetic force theorem (Lichtenstein, Katsnelson, Antropov, Gubanov
JMMM 1987)

Calculations: Uppsala team (Olle Eriksson group)



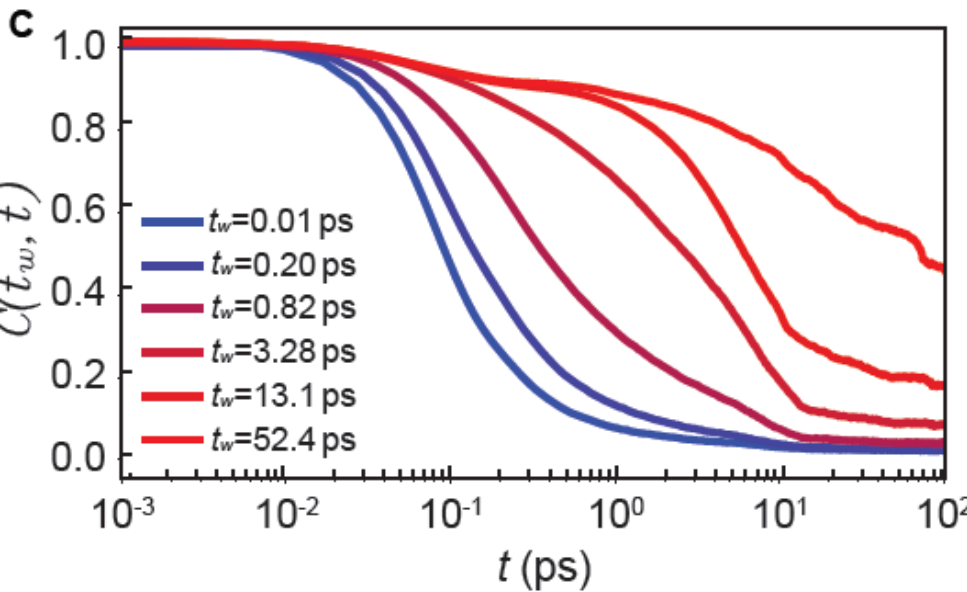
- Dhcp structure drives competing AFM interactions
- Frustrated magnetism

Ab initio bulk Nd: energy landscape



- $E(Q)$ landscape features flat valleys along high symmetry directions

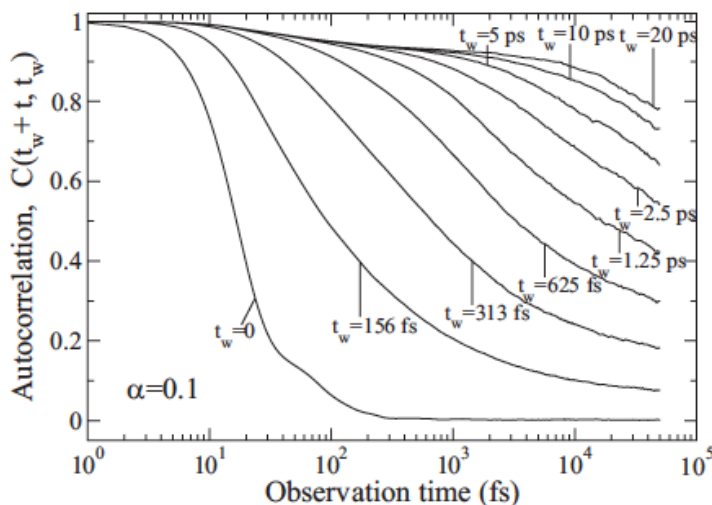
Spin-glass state in Nd: spin dynamics



Atomistic spin dynamics simulations

Typically spin-glass behavior

Autocorrelation function $C(t_w, t) = \langle \mathbf{m}_i(t + t_w) \cdot \mathbf{m}_i(t_w) \rangle$ for dhcp Nd at $T = 1$ K



To compare: the same for prototype *disordered* spin-glass Cu-Mn

B. Skubic et al, PRB 79, 024411 (2009)

Order from disorder

Thermally induced magnetic order from glassiness in elemental neodymium

NATURE PHYSICS | VOL 18 | AUGUST 2022 | 905-911

Benjamin Verlhac¹, Lorena Niggli¹, Anders Bergman², Umut Kamber¹, Andrey Bagrov^{1,2}, Diana Iuşan², Lars Nordström¹, Mikhail I. Katsnelson¹, Daniel Wegner¹, Olle Eriksson^{2,3} and Alexander A. Khajetoorians¹

Glassy state at low T
and long-range order
at T increase

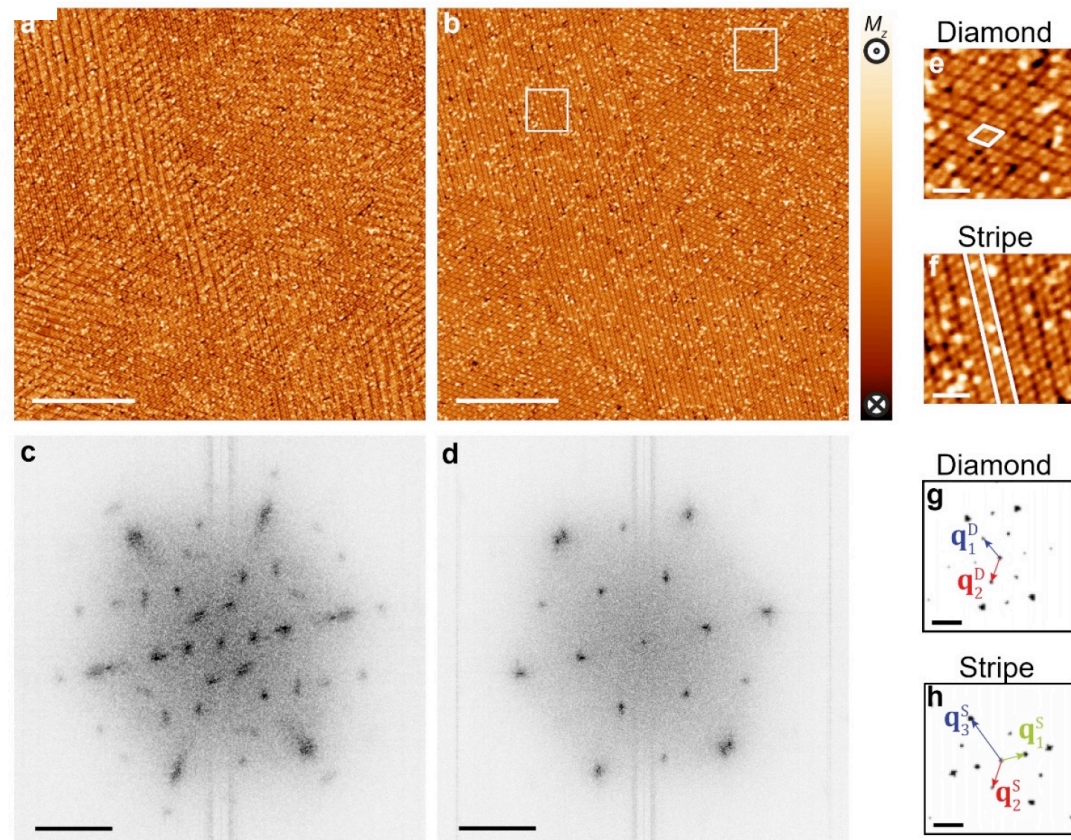
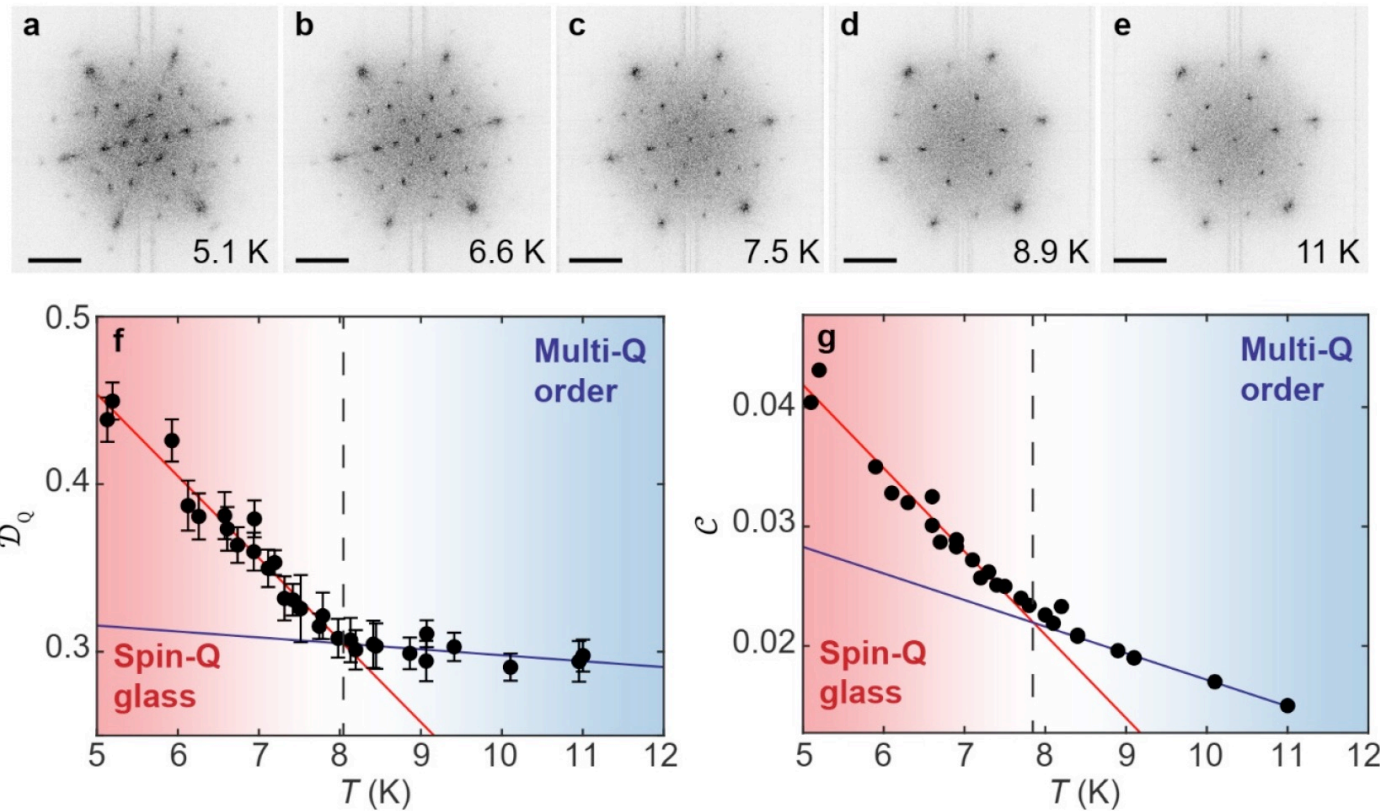


Figure 2: Emergence of long-range multi-Q order from the spin-Q glass state at elevated temperature. a,b. Magnetization images of the same region at $T = 5.1$ K and 11 K, respectively ($I = 100$ pA, a-b, scale bar: 50 nm). c,d. Corresponding Q-space images (scale bars: 3 nm $^{-1}$), illustrating the changes from strong local (i.e. lack of long-range) Q order toward multiple large-scale domains with well-defined long-range multi-Q order. e,f. Zoom-in images of the diamond-like (e) and stripe-like (f) patterns (scale bar: 5 nm). The locations of these images is shown by the white squares in b,g,h. Display of multi-Q state maps of the two apparent domains in the multi-Q ordered phase, where (g)

$T=5$ K (a,c): spin glass
 $T=11$ K(b,d): (noncollinear) AFM

Order from disorder II



Phase transition at approx. 8K (seen via “complexity” measures) – right one is our multiscale structural complexity!

Frustrations and complexity: Quantum case

Generalization properties of neural network

NATURE COMMUNICATIONS | (2020)11:1593

approximations to frustrated magnet ground states

Tom Westerhout¹✉, Nikita Astrakhantsev^{2,3,4}✉, Konstantin S. Tikhonov^{5,6,7}✉, Mikhail I. Katsnelson^{1,8} & Andrey A. Bagrov^{1,8,9}✉

How to find true ground state of the quantum system?

In general, a very complicated problem (difficult to solve even for quantum computer!)

Idea: use of variational approach and train neural network to find “the best” trial function (**G. Carleo and M. Troyer, Science 355, 602 (2017)**)

$$|\Psi_{\text{GS}}\rangle = \sum_{i=1}^K \psi_i |\mathcal{S}_i\rangle = \sum_{i=1}^K s_i |\psi_i\rangle |\mathcal{S}_i\rangle$$

Generalization problem: to train NN for relatively small basis (K much smaller than total dim. of quantum space) and find good approximation to the true ground state

Frustrations and complexity: Quantum case II

Quantum $S=1/2$ Hamiltonian
NN and NNN interactions

$$\hat{H} = J_1 \sum_{\langle a,b \rangle} \hat{\sigma}_a \otimes \hat{\sigma}_b + J_2 \sum_{\langle \langle a,b \rangle \rangle} \hat{\sigma}_a \otimes \hat{\sigma}_b$$

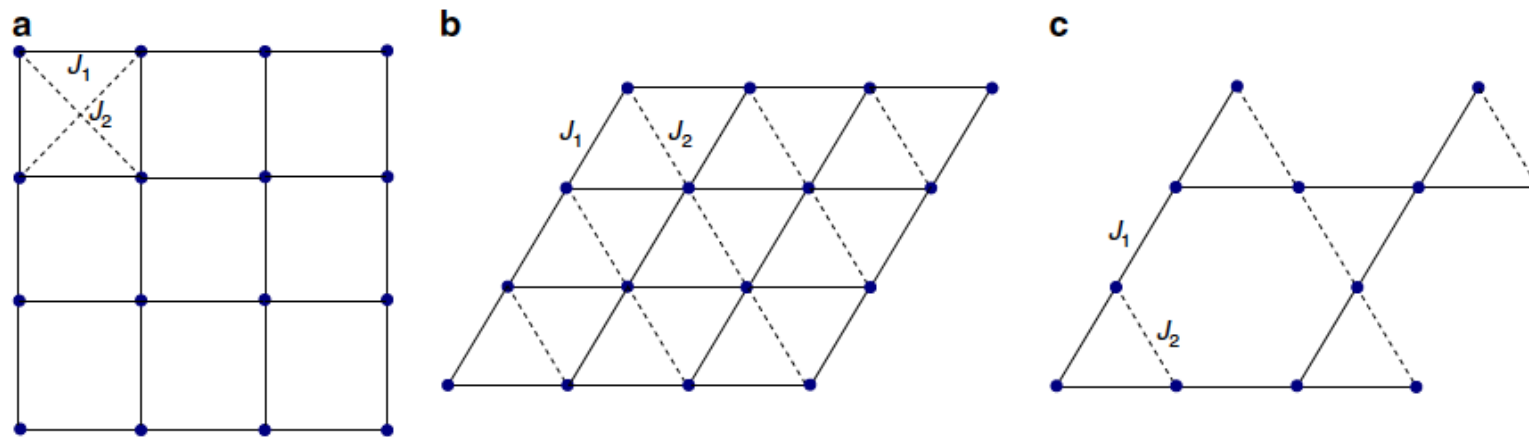


Fig. 1 Lattices considered in this work. We studied three frustrated antiferromagnetic Heisenberg models: **a** next-nearest neighbor J_1 – J_2 model on square lattice; **b** anisotropic nearest-neighbor model on triangular lattice; **c** spatially anisotropic Kagome lattice. In all cases $J_2 = 0$ corresponds to the absence of frustration.

24 spins, dimensionality of Hilbert space $d = C_{12}^{24} \simeq 2.7 \cdot 10^6$

Still possible to calculate ground state exactly
Training for $K = 0.01$ d (small trial set)

Frustrations and complexity: Quantum case III

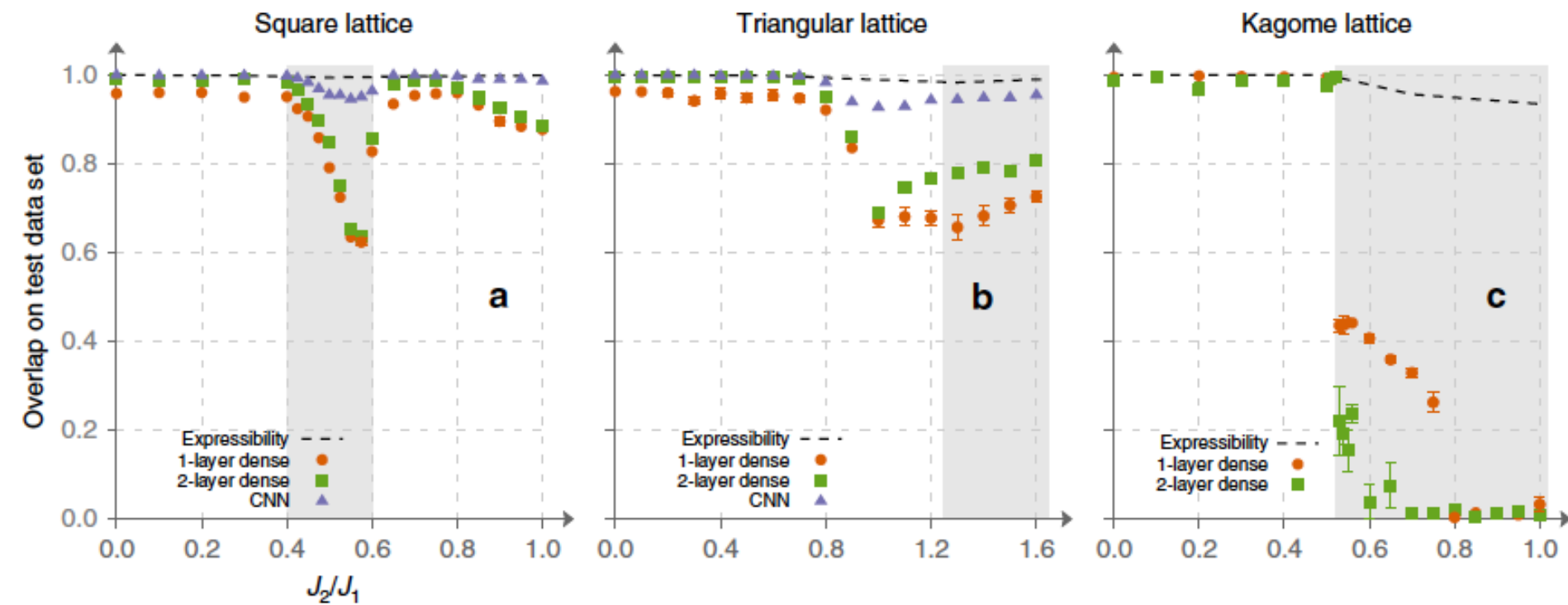
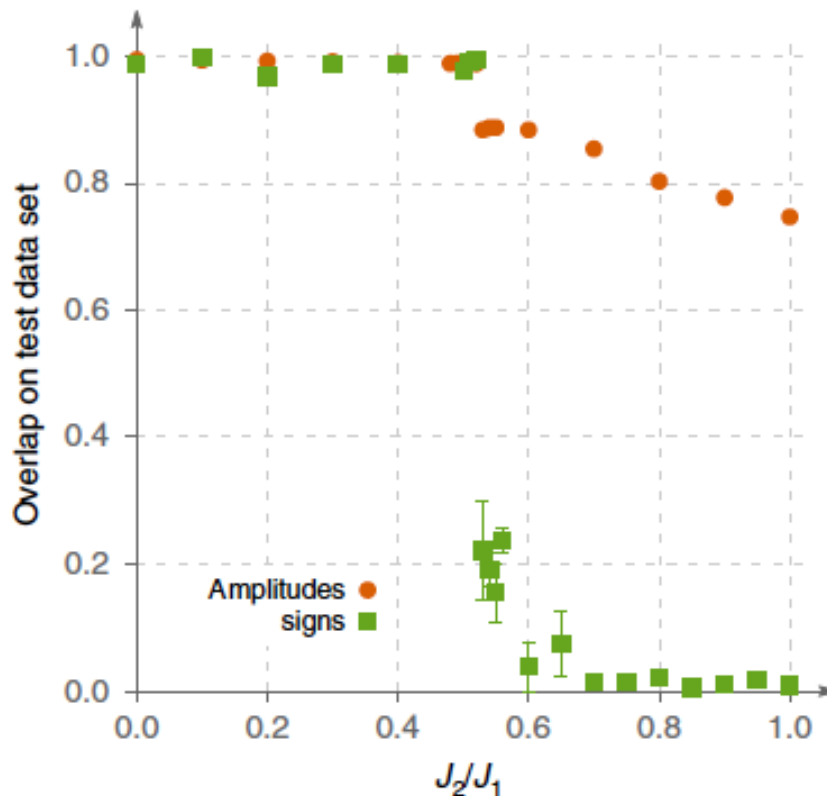


Fig. 2 Optimization results for 24-site clusters obtained with supervised learning and stochastic reconfiguration. Subfigures **a-c** were obtained using supervised learning of the sign structure. Overlap of the variational wave function with the exact ground state is shown as function of J_2/J_1 for square **a**, triangular **b**, and Kagome **c** lattices. Overlap was computed on the test dataset (not included into training and validation datasets). Note that generalization is poor in the frustrated regions (which are shaded on the plots). 1-layer dense, 2-layer dense, and convolutional neural network (CNN) architectures are described in Supplementary Note 1. Subfigures **d-f** show overlap between the variational wave function optimized using Stochastic Reconfiguration and the exact ground state for square, triangular, and Kagome lattices, respectively. Variational wave function was represented by two two-layer dense networks. A correlation between generalization quality and accuracy of the SR method is evident. On this figure, as well as on all the subsequent ones (both in the main text and Supplementary Notes 1 and 2), error bars represent standard error (SE) obtained by repeating simulations multiple times.

Frustrations and complexity: Quantum case IV



It is *sign* structure
which is difficult to
learn in frustrated
case!!!

Relation to sign
problem in QMC?!

Fig. 4 Generalization of signs and amplitudes. We compare generalization quality as measured by overlap for learning the sign structure (red circles) and amplitude structure (green squares) for 24-site Kagome lattice for two-layer dense architecture. Note that both curves decrease in the frustrated region, but the sign structure is much harder to learn.

"Somehow it seems to fill my head with ideas –only I don't exactly know what they are!" (Through the Looking-Glass, and What Alice Found There)

Further development

Many-body quantum sign structures as non-glassy Ising models

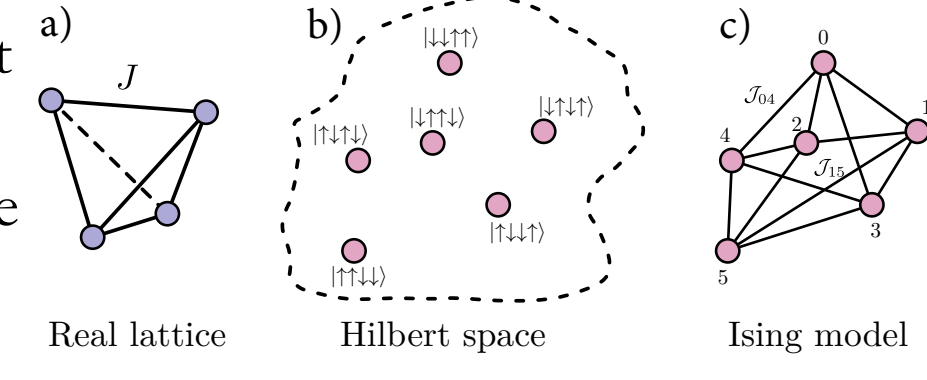
Tom Westerhout, Mikhail I. Katsnelson, Andrey A. Bagrov

Communications Physics volume 6, Article number: 275 (2023)

The idea: use machine learning to find amplitudes and then map onto efficient Ising model

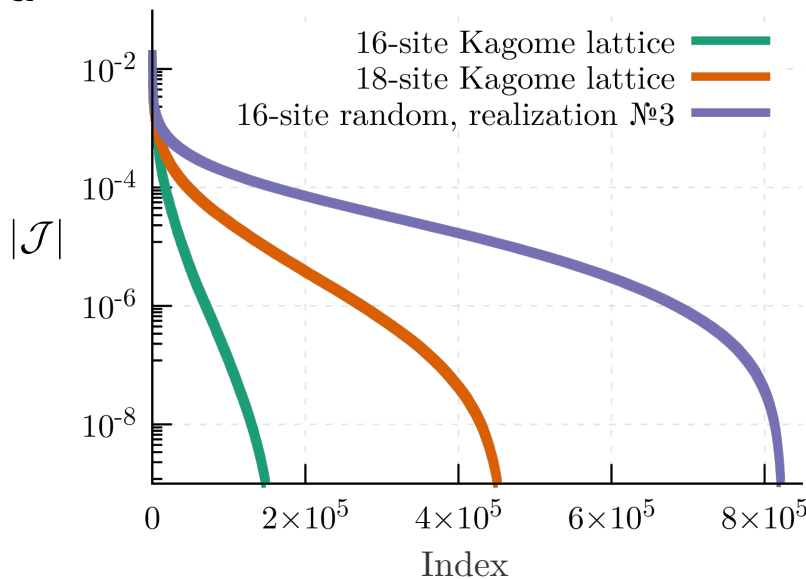
$$|\Psi_{\text{GS}}\rangle = \sum_{i=1}^K \psi_i |\mathcal{S}_i\rangle = \sum_{i=1}^K s_i |\psi_i\rangle |\mathcal{S}_i\rangle$$

When amplitudes are known the trial ground state energy $\langle \Psi | H | \Psi \rangle$ is a bilinear function of signs s_i , and we have Ising optimization problem in K -dimensional space; K is very big but it turns out that the model is not glassy and can be optimized without too serious problems

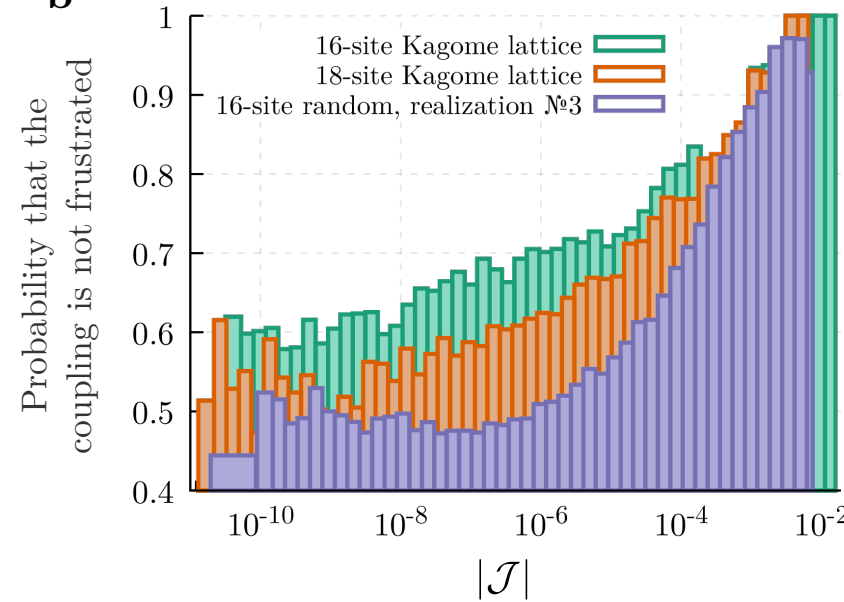


Further development II

a

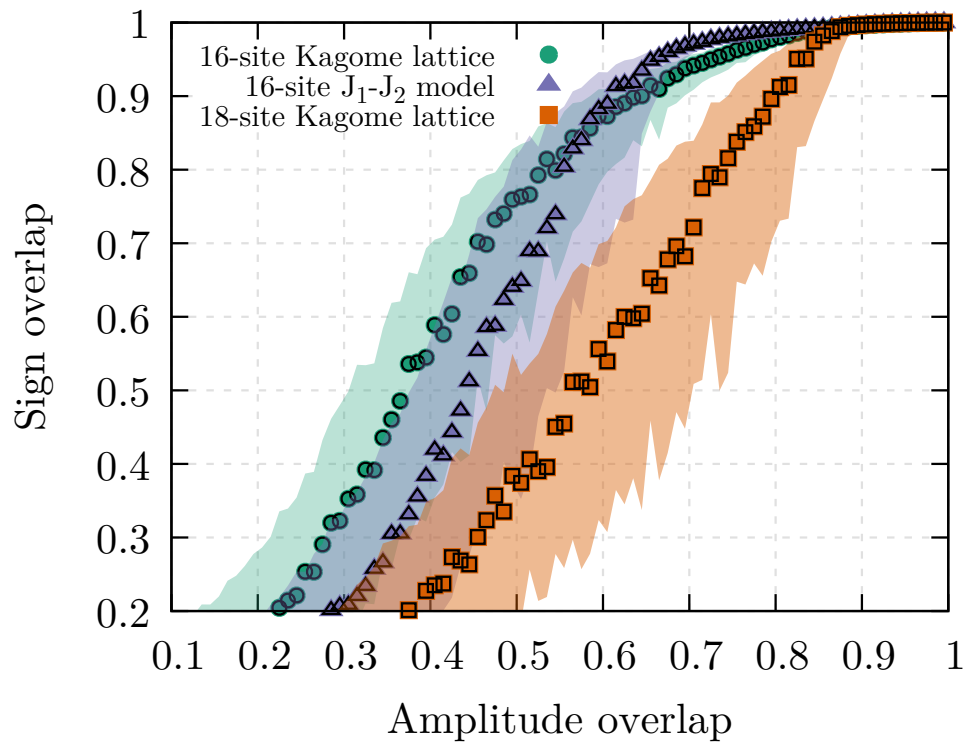


b



It turns out that even for initially frustrated quantum spin models the effective Ising model is not frustrated, both couplings are small and optimization is quite efficient

Further development III



The quality of optimization is quite robust with respect to uncertainties in amplitudes (overlap with the exact ground state)

Analogy with biological evolution?

Toward a theory of evolution as multilevel learning

Vitaly Vanchurin^{a,b,1}, Yuri I. Wolf^a , Mikhail I. Katsnelson^c , and Eugene V. Koonin^{a,1} 

PNAS 2022 Vol. 119 No. 6 e2120037119

Thermodynamics of evolution and the origin of life

Vitaly Vanchurin^{a,b,1}, Yuri I. Wolf^a , Eugene V. Koonin^{a,1} , and Mikhail I. Katsnelson^{c,1} 

PNAS 2022 Vol. 119 No. 6 e2120042119

Table 1. Corresponding quantities in thermodynamics, machine learning, and evolutionary biology

	Thermodynamics	Machine learning	Evolutionary biology
x	Microscopic physical degrees of freedom	Variables describing training dataset (nontrainable variables)	Variables describing environment
q	Generalized coordinates (e.g., volume)	Weight matrix and bias vector (trainable variables)	Trainable variables (genotype, phenotype)
$H(x, q)$	Energy	Loss function	Additive fitness, $H(x, q) = -T \log f(q)$
$S(q)$	Entropy of physical system	Entropy of nontrainable variables	Entropy of biological system
$U(q)$	Internal energy	Average loss function	Average additive fitness
$Z(T, q)$	Partition function	Partition function	Macroscopic fitness
$F(T, q)$	Helmholtz free energy	Free energy	Adaptive potential (macroscopic additive fitness)
$\Omega(T, \mu)$	Grand potential, $\Omega_p(\mathcal{T}, \mathcal{M})$	Grand potential	Grand potential, $\Omega_b(T, \mu)$
T or \mathcal{T}	Physical temperature, \mathcal{T}	Temperature	Evolutionary temperature, T
μ or \mathcal{M}	Chemical potential, \mathcal{M}	Absent in conventional machine learning	Evolutionary potential, μ
N_e or N	Number of molecules, N	Number of neurons, N	Effective population size, N_e
K	Absent in conventional physics	Number of trainable variables	Number of adaptable variables

Energy landscape in physics is similar to fitness landscape in biology

Analogy with biological evolution II

Can the change of e.g. biological temperature switch fitness landscape from a few well-defined peaks to a glassy-like with many directions of possible evolution?

Explaining the Cambrian “Explosion” of Animals

Charles R. Marshall

Annu. Rev. Earth Planet. Sci.
2006. 34:355–84

Australian Journal of Zoology
<http://dx.doi.org/10.1071/ZO13052>

The evolution of morphogenetic fitness landscapes: conceptualising the interplay between the developmental and ecological drivers of morphological innovation

Charles R. Marshall

Cambrian Explosion as an analog of magnetic phase transitions in neodymium?!

Well... for me (as a physicist) it is a good place to stop

**MANY THANKS FOR YOUR
ATTENTION**